Cell Host & Microbe
Short Article

Shigella Effector IpaB-Induced Cholesterol Relocation Disrupts the Golgi Complex and Recycling Network to Inhibit Host Cell Secretion

Joëlle Mounier,[1,2] Gaëlle Boncompain,[6,7,13] Lidija Senerovic,[8,13,15] Thibault Lagache,[5,9,13] Fabrice Chrétien,[10,11,12] Franck Perez,[6,7] Michael Kolbe,[8] Jean-Christophe Olivo-Marin,[5,9] Philippe J. Sansonetti,[1,2,3,14,*] and Nathalie Sauvonnet[4,5,14,*]

[1]Institut Pasteur, Unité de Pathogénie Microbienne Moléculaire, 28 rue du Docteur Roux, 75724 Paris Cedex 15, France
[2]INSERM, Unité 786, Institut Pasteur, Cedex 15, France
[3]Collège de France, 11 Place Marcellin Berthelot, 75005 Paris Cedex 15, France
[4]Institut Pasteur, Unité de Biologie des Interactions Cellulaires, 25 rue du Docteur Roux, 75724 Paris Cedex 15, France
[5]CNRS URA 2582, 75724 Paris Cedex 15, France
[6]Institut Curie, Centre de Recherche, 26 rue d'Ulm, 75248 Paris Cedex 15, France
[7]CNRS UMR144, 75248 Paris, France
[8]Max Planck Institute for Infection Biology, Charitéplatz 1, 10117 Berlin, Germany
[9]Institut Pasteur, Unité d'Analyse d'Images Quantitative, 25 rue du Docteur Roux, 75724 Paris Cedex 15, France
[10]Institut Pasteur, Unité d'Histopathologie humaine et modèles animaux, 25 rue du Docteur Roux, 75724 Paris Cedex 15, France
[11]Faculté de Médecine, Université Versailles Saint Quentin en Yvelines, France
[12]Service d'Anatomie Pathologique, AP-HP, Hôpital R. Poincaré, France
[13]These authors contributed equally to this work
[14]These authors contributed equally to this work
[15]Present address: Laboratory for Microbial Molecular Genetics and Ecology, Institute of Molecular Genetics and Genetic Engineering, University of Belgrade, Vojvode Stepe 444a, PO Box 23, 11010 Belgrade, Serbia
*Correspondence: nathalie.sauvonnet@pasteur.fr (N.S.), philippe.sansonetti@pasteur.fr (P.J.S.)
http://dx.doi.org/10.1016/j.chom.2012.07.010

SUMMARY

Shigella **infection causes destruction of the human colonic epithelial barrier. The Golgi network and recycling endosomes are essential for maintaining epithelial barrier function. Here we show that *Shigella* epithelial invasion induces fragmentation of the Golgi complex with consequent inhibition of both secretion and retrograde transport in the infected host cell. *Shigella* induces tubulation of the Rab11-positive compartment, thereby affecting cell surface receptor recycling. The molecular process underlying the observed damage to the Golgi complex and receptor recycling is a massive redistribution of plasma membrane cholesterol to the sites of *Shigella* entry. IpaB, a virulence factor of *Shigella* that is known to bind cholesterol, is necessary and sufficient to induce Golgi fragmentation and reorganization of the recycling compartment. *Shigella* infection-induced Golgi disorganization was also observed in vivo, suggesting that this mechanism affecting the sorting of cell surface molecules likely contributes to host epithelial barrier disruption associated with *Shigella* pathogenesis.**

INTRODUCTION

Shigella invasion of epithelial cells depends on the translocation of around 30 effector proteins into the membrane and cytosol of its target cells through a Type III Secretion System (T3SS). Two of these, IpaB and IpaC get inserted into the host cell plasma membrane to allow injection of effector proteins (Parsot, 2009). The C-terminal domain of IpaC, which becomes exposed to the cell cytoplasm, triggers the actin rearrangements that allow bacterial uptake. The effectors injected into the cytoplasm affect an array of functions such as reorganizing the actin cytoskeleton or modulating cell-signaling pathways to inhibit innate immune responses (Ashida et al., 2009; Phalipon and Sansonetti, 2007). The initial site of *Shigella* infection is the epithelium and invasion triggers the inflammatory destruction of the gut barrier. Its success as a pathogen resides in its capacity to colonize the intestinal epithelium by subverting essential functions of epithelial cells while proceeding to their invasion (Sansonetti, 2006). The Golgi network and recycling endosomes play an essential role on the sorting of surface molecules and thus are crucial for the differentiation and maintenance of the barrier functions of the epithelium. We report that *Shigella* invasion induces major alteration of the recycling pathway and severe damage to the Golgi complex in response to cholesterol redistribution. IpaB, an essential virulence factor of *Shigella* known to bind cholesterol, is necessary and sufficient to induce Golgi fragmentation and reorganization of the recycling compartment.

RESULTS

Shigella Affects the Recycling Compartment

To test the effect of *Shigella* infection on recycling endosomes, we used a wild-type invasive isolate (M90T) and an invasion-deficient mutant in the T3SS (*mxiD*) to infect the human epithelial cell line Hep2β. After 15 min of incubation, a sufficient time to

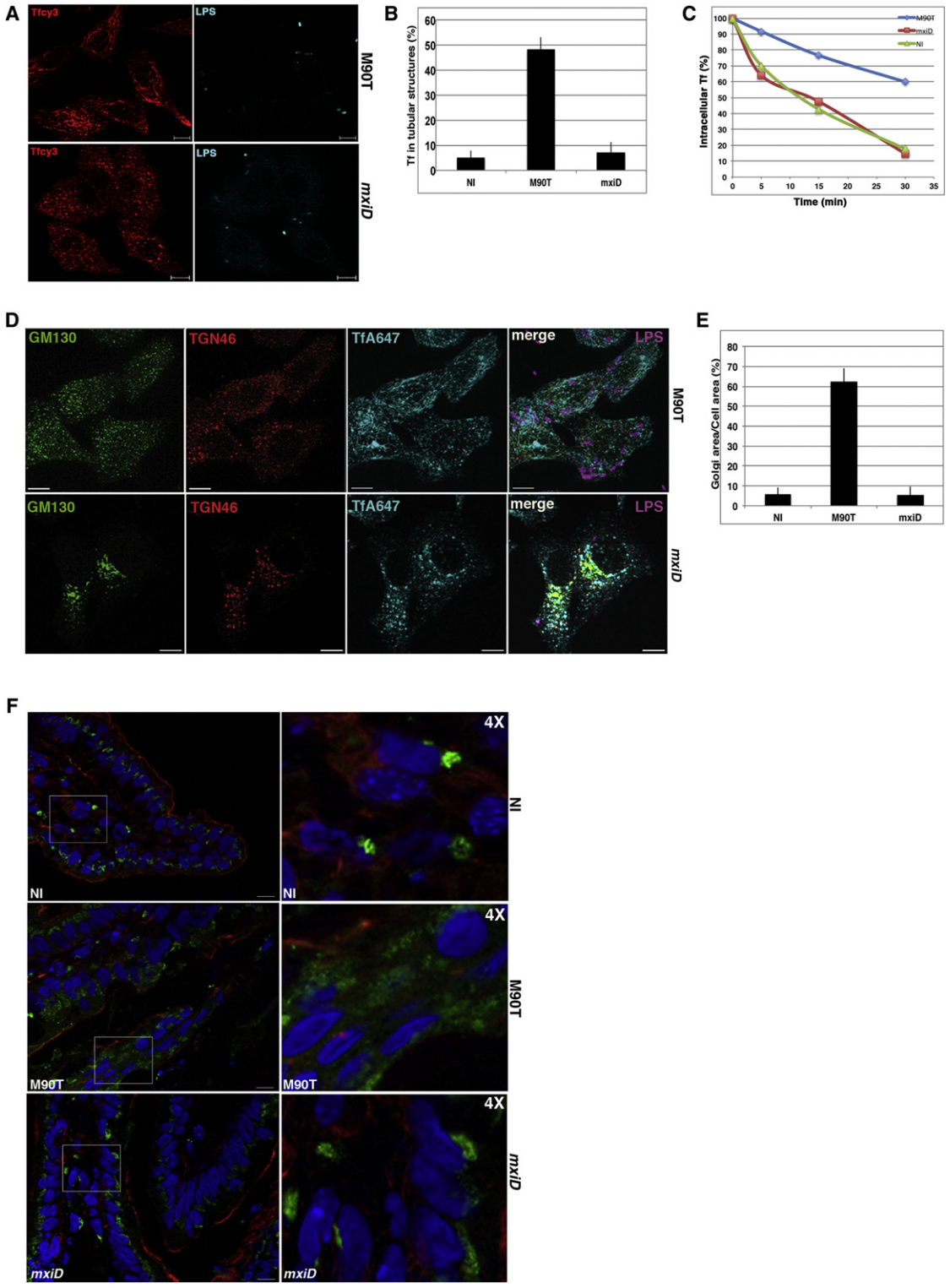

Figure 1. *Shigella* Affects the Recycling Endosomes and the Golgi Complex

(A) Hep2β cells were infected with M90T or *mxiD* bacteria for 15 min at 37°C, and Tfcy3 was added for another 30 min at 37°C. Cells were then fixed, permeabilized, and *Shigella* labeled with an anti-LPS.

(B) Quantification using ICY software of the data presented in (A), where the amounts of tubulated Tf were expressed as a percentage of Tf objects (mean ± S.E.; n = 25).

(C) Hep2β cells either noninfected (NI, triangle) or infected with M90T (diamond) or *mxiD* (square) bacteria were used to follow Tf recycling by performing pulse chase experiment monitoring the intracellular TfA647 by FACS.

complete entry of wild-type *Shigella*, we added transferrin (Tf) coupled to the cy3 fluorochrome (Tfcy3), a recycling marker that is endocytosed by a clathrin-mediated pathway, and recycles back to the plasma membrane. Cells were then fixed, permeabilized, and bacteria were stained with an anti-LPS antibody (Figure 1A). After 45 min of infection, we observed the formation of a tubular compartment containing Tf in M90T-infected cells, whereas Tf appeared in vesicular structures in *mxiD*- and noninfected (NI) cells (Figures 1A and S1A). To quantify this effect, we developed a plugin for ICY imaging software allowing quantification of tubular versus nontubular structures (Supplemental Information). In M90T-infected cells around 50% of Tf was in tubules, in contrast to *mxiD*- or noninfected cells where only 5% was in tubules (Figure 1B). Tubulation was visible in all infected cells and remained stable at least until 4 hr of infection. To determine the nature of these tubular compartments, we transfected Hep2β cells with either Green Fluorescent Protein (GFP)-tagged Rab11 or GFP-tagged Rab4, infected them with M90T or *mxiD* bacteria and incubated them with Tfcy3 as above. Rab11- and Tf-positive compartments became tubular in M90T-infected cells, but not in *mxiD*-infected cells (Figure S1B). In contrast, Rab4 was not found in tubules in M90T-infected cells (Figure S1B). The quantification of the data using ICY software, showed that in M90T-infected cells, 57% of Rab11 was organized in tubular structures, whereas only 5.5% of Rab4 was in such structures (Figure S1C). We next analyzed the impact of *Shigella* infection on the kinetics of Tf recycling by pulse chase experiments (Coumailleau et al., 2004), using Fluorescence Activated Cell Sorting (FACS) on Hep2β NI, M90T- or *mxiD*-infected cells (Figure 1C and Supplemental Information). We observed a 50% reduction of Tf recycling in M90T-infected cells compared to NI or *mxiD*-infected cells (Figure 1C). These data demonstrate that *Shigella* strongly affects the Rab11-positive perinuclear recycling compartment, leading to the inhibition of Tf recycling.

Shigella Induces Fragmentation of the Golgi Complex In Vitro and In Vivo

We then investigated the effect of *Shigella* infection on the Golgi complex. Hep2β cells were infected with M90T or *mxiD* bacteria for 15 min and Tf coupled to AlexaFluor647 (TfA647) was added and incubated at 37°C for 30 min. Cells were then fixed, permeabilized, and processed for immunofluorescence. The *cis*-Golgi complex was labeled with an anti-GM130 antibody, the Trans Golgi Network (TGN) was labeled with an anti-TGN46 antibody, and bacteria with an anti-LPS antibody (Figure 1D). We observed a total fragmentation of the *cis*-Golgi and TGN that appeared dispersed throughout the cell cytoplasm in M90T-infected cells. In contrast, the Golgi apparatus was more compact in *mxiD*- and noninfected (NI) cells (Figures 1D and S1A). To quantify this phenotype we developed another plugin in ICY software that measures the area covered by the Golgi complex normalized to the cell area (Supplemental Information). In M90T-infected cells the Golgi covered around 60% of the cell area whereas in *mxiD*- or noninfected (NI) cells it was restricted to 5% of the cell area (Figure 1E). The Golgi fragmentation induced by *Shigella* M90T appeared as quickly as 20 min post infection and remained stable for several hours as shown in the Movie S1. Importantly, microtubules were not disassembled in cells infected with M90T bacteria.

We then tested the effect of *Shigella* infection on the Golgi complex in vivo, by using human fetal intestinal xenotransplants that were subsequently infected either with M90T or *mxiD* strains of *Shigella* during 4 hr, in comparison with noninfected tissues (Sperandio et al., 2008). Following euthanasia, intestinal segments were collected, fixed and processed for histopathological analysis. Fluorescence labeling was carried out on sections embedded on coverslips, i.e., Hoechst staining for nucleus and phalloidin-TRITC for the actin cytoskeleton, and immunofluorescence staining with relevant antibodies for the Golgi complex (Figure 1F and Supplemental Information). M90T disorganized the epithelium in vivo. Cells lost their cylindrical, linear and regular aspect, some presented with a more cuboïdal shape, inducing a scalloped aspect of the villi (Figure 1F). Strikingly, the Golgi distribution was affected by M90T infection (Figure 1F). In *mxiD*- or noninfected tissues, the Golgi complex was clustered adjacent to the nucleus whereas a diffuse Golgi labeling was seen upon M90T infection (Figure 1F). This result shows that *Shigella* infection leads to Golgi dispersion in vivo.

Shigella Impairs Anterograde and Retrograde Transport through the Golgi Complex

To assess whether the Golgi complex was still competent for anterograde trafficking upon *Shigella* infection, we analyzed the secretion at the plasma membrane of E-cadherin, a key molecule for the maintenance of the epithelium barrier. Traffic of E-cadherin was monitored by the RUSH system (Retention Using Selective Hooks, (Boncompain et al., 2012). E-cadherin is fused to a SBP (Streptavidin Binding Peptide) and EGFP tags and coexpressed with Streptavidin-KDEL, which is stably localized in the endoplasmic reticulum (ER) (Boncompain et al., 2012). At steady state, SBP-EGFP-E-cadherin interacts with Streptavidin-KDEL in the ER preventing its transport to the plasma membrane (see "retained" in Figure S2A). After addition of biotin, which competes out the SBP tag, SBP-EGFP-E-cadherin is released from Streptavidin-KDEL and trafficked synchronously through the Golgi complex toward the plasma membrane in NI cells and cells infected with *mxiD* (Figures 2A and S2A). In contrast, in cells infected with the M90T strain, E-cadherin molecules remained in the ER upon addition of biotin and did not reach the plasma membrane (Figure 2A). The quantification of the data revealed a drastic 3-fold reduction in the amount of surface located E-cadherin in M90T-infected cells in contrast to the *mxiD*- or noninfected cells (Figure 2B). Interestingly, we could not see any effect of *Shigella* on the overall ER morphology.

(D and E) Hep2β cells were infected with M90T or *mxiD* bacteria for 15 min at 37°C, and TfA647 was added for 30 min at 37°C. After fixation and permeabilization, cells were labeled with anti-GM130, anti-TGN46 and anti-LPS. (E) shows quantification of the Golgi area using ICY on data presented in (D). The Golgi area is measured using GM130 labeling and expressed as a percentage of total cell area (mean ± S.E.; n = 25).

(F) *Shigella* induces Golgi dispersion in vivo in intestinal epithelium of animals. Human intestinal xenografts in mouse infected by M90T, *mxiD*, or NI during 4 hr were subjected to immunofluorescence experiment labeling actin (Phalloidin-TRITC in red), nucleus (Hoechst in blue), and Golgi (anti-Golim4 in green); images are shown enlarged 4 times. Scale bars represent 10 μm. (See also Figure S1.)

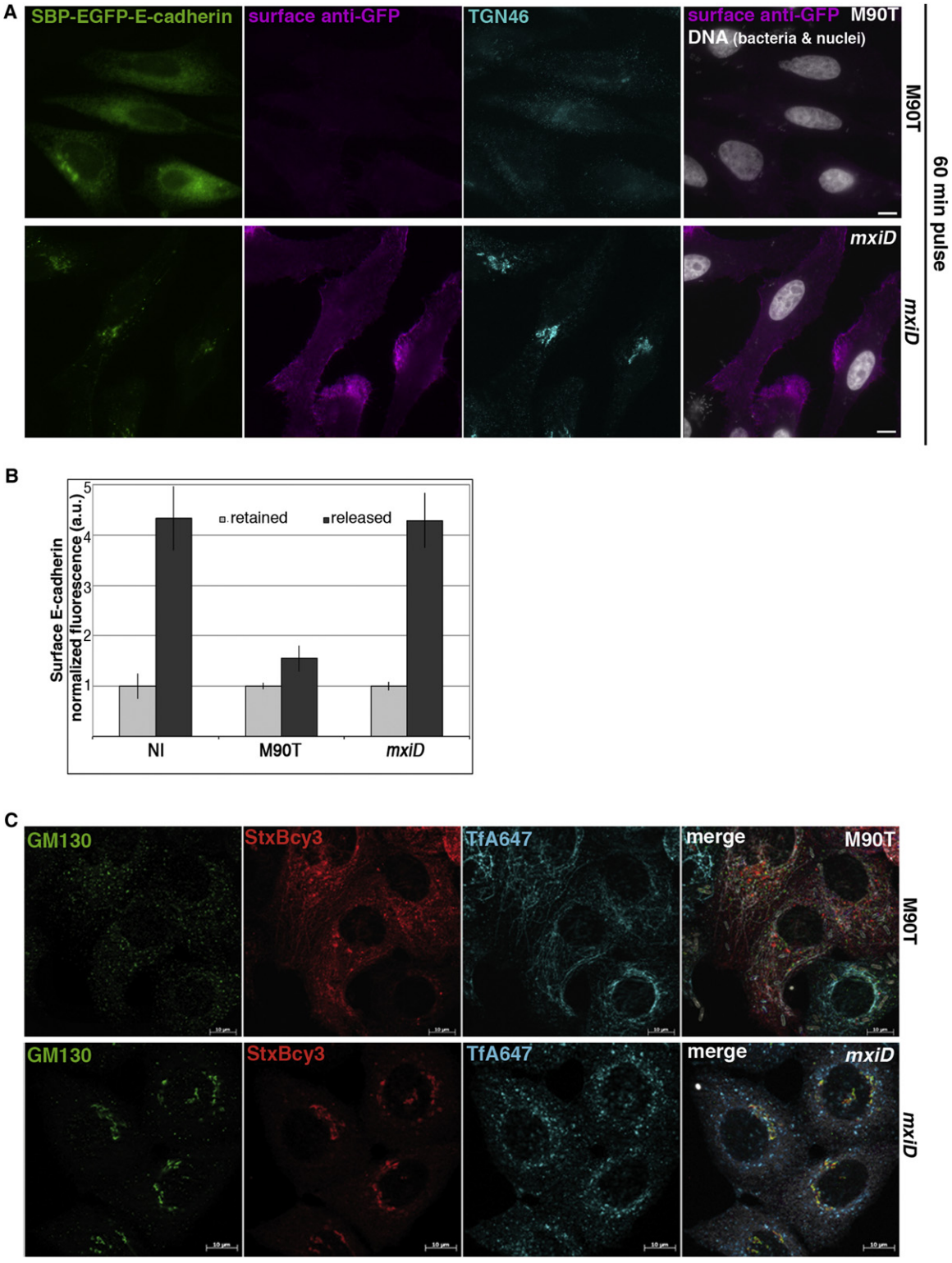

Figure 2. *Shigella* Affects Golgi Function

(A) Anterograde trafficking is inhibited in *Shigella* infected cells. HeLa cells expressing the RUSH proteins: Streptavidin-KDEL and SBP-EGFP-E-cadherin were infected with M90T or *mxiD* bacteria. Cells were then incubated for 60 min at 37°C with biotin to observe the traffic of SBP-EGFP-E-cadherin toward the plasma membrane (60 min pulse). Cells were then fixed and the surface E-cadherin was detected with an anti-GFP (magenta) prior to cell permeabilization. After permeabilization, the Golgi apparatus was stained using an anti-TGN46 antibody (cyan); bacteria (and cell nuclei) were visualized using DAPI staining (white on merge). Scale bars represent 5 μm.

Next, we tested whether the retrograde transport was affected by *Shigella* invasion. We analyzed the traffic of the Gb3-binding B-subunit of Shiga toxin coupled to cy3 (StxBcy3) that we used as a bona fide marker of the retrograde transport (Johannes and Römer, 2010; Mallard et al., 1998). We first incubated Hep2β cells with StxBcy3 for 1h at 19.5°C to let the toxin accumulate in early endosomes. Then, cells were infected with M90T or *mxiD* bacteria for 15 min at 37°C. TfA647 was then added and cells were further incubated at 37°C. Cells were then fixed, permeabilized and GM130 and LPS were labeled as previously described (Figure 2C and Supplemental Information). After 15 min of infection by M90T-, *mxiD*-bacteria, as well as in NI cells, StxBcy3 reached the Golgi apparatus that displayed a normal morphology in the three conditions (Figure S2B). After 75 min of *mxiD* infection, StxBcy3 was also found in the compact and centrally localized GM130-positive Golgi complex (Figure 2C). Strikingly, in M90T-infected cells, the Golgi complex appeared fragmented and StxBcy3 did not colocalize with GM130 vesicles but was mainly found associated to TfA647-positive tubules (Figure 2C). We observed that StxBcy3 was in tubules even after 120 min of M90T infection (Figure S2C). In addition, we analyzed the transport of StxBcy3 into the ER after 120 min of infection and observed the presence of StxBcy3 in calnexin-positive ER structures in *mxiD*- and noninfected cells. StxBcy3 was not detected in the ER of M90T-infected cells (Figure S2C). Thus, StxB did not reach the GM130-positive Golgi fragments in M90T-infected cells but was rerouted to the tubular recycling endosomes.

Identification of the *Shigella* Effector Causing the Reorganization of the Golgi-Recycling Network

A T3SS-mutated strain (*mxiD*) or a translocator-mutated strain (*ipaB* or *ipaC*) that are unable to deliver virulence effectors did not affect the Golgi complex or the recycling networks upon infection (Table S1). To determine if one of the effectors injected by *Shigella* was responsible for the Golgi dispersion and recycling inhibition, we tested a battery of *Shigella* mutants affected in expression of individual effector proteins or in the master regulator *mxiE* (Table S1). All mutated strains induced tubulation of endosomes and Golgi fragmentation (Table S1). VirA is not involved in Golgi fragmentation although ectopic expression of a homologous protein from *enteropathogenic/hemorrhagic Escherichia coli* (EPEC or EHEC), EspG, was shown to affect the Golgi complex (Clements et al., 2011; Selyunin et al., 2011). Altogether, these data indicated that the relevant effector was likely to be a structural element of the TTSS, or the translocator (*i.e.* IpaB, C and D).

Cholesterol Delocalization by *Shigella* Entry Is Involved in the Golgi-Recycling Reorganization

A key factor of *Shigella* invasion is plasma membrane cholesterol (Lafont et al., 2002). It controls the insertion of the translocator (IpaB, IpaC), via IpaB-cholesterol interaction (Epler et al., 2009; Hayward et al., 2005). Cholesterol is a key player in intracellular trafficking (Lippincott-Schwartz and Phair, 2010). Eukaryotic cells maintain a gradient in cholesterol concentration, with the ER having a low concentration, the Golgi having an intermediate concentration and the plasma membrane having the highest concentration (Mesmin and Maxfield, 2009). This gradient of cholesterol concentration is essential for endomembranes and an imbalance of cholesterol in the Golgi complex leads to its fragmentation (Lebreton et al., 2008; Simons and Ehehalt, 2002). Following overloading or depletion of cholesterol in Hep2β cells we observed a Golgi disruption that spanned around 60% of the cell area (Supplemental Information, Figures S3A and S3B). Therefore, proper cholesterol balance among the membranes embracing the various cell compartments and organelles is necessary to maintain the Golgi complex. Although depletion or overloading of cholesterol did not lead to a typical tubulation of recycling endosomes, Tf-positive vesicles appeared much bigger (1.6 to 2 times, as determined by ICY software) than those observed in non treated cells (Figure S3C). We then tested whether *Shigella* modified the cholesterol distribution in infected cells. At early times of infection, when *Shigella* induced actin recruitment for its entry (until 20 min of infection), we observed a massive delocalization of cholesterol, labeled by filipin, in actin-containing foci (Figure 3A). In contrast, *mxiD*-infected cells showed a strictly balanced distribution of cholesterol, visible in the Golgi complex and at the plasma membrane (Figure 3A). We then tried to antagonize Golgi fragmentation and Tf tubulation by adding cholesterol to cells 30 min after their infection with M90T. In the presence of additional cholesterol, Tf was partly localized in vesicular structures as only 28% of Tf was in tubules in contrast to 50% in M90T-infected control cells (Figures 3B and 3D). Moreover, the Golgi complex was more compact after cholesterol addition as it covered 30% of the cell area in contrast to 62% in M90T-infected cells (Figures 3B and 3E). The addition of cholesterol thus decreased the tubulation of recycling endosomes and the scattering of the Golgi complex. However, the reversion was not total since in NI cells we observed only 5% of Tf in tubules and the Golgi area represented about 6% of the cell area (Figure S3B). To further test for cholesterol-mediated reversion, we looked at the retrograde transport of StxBcy3 in M90T-infected cells incubated or not with cholesterol (Figure 3C). In agreement with the phenotypical reversion observed above, the addition of cholesterol in M90T-infected cells restored proper trafficking of StxBcy3 that was able to reach the now more compact Golgi complex (Figures 3C and 3E).

The Translocator Protein IpaB Causes the Reorganization of the Golgi and Recycling Networks

Because the translocator protein IpaB directly binds to cholesterol, we analyzed its role on intracellular membrane perturbation by incubating cells with the purified protein (Figure S4). After 90 min of incubation with 400 nM of purified protein, IpaB appeared distributed at the cell surface and inside Hep2β cells (Figure 4A). It led to the clear redistribution of cholesterol,

(B) Quantification of surface E-cadherin in cells noninfected (NI) or infected with M90T or *mxiD* using anti-GFP immunolabeling. Average intensity of regions of interest corresponding to transfected cells was measured and normalized by the values obtained for the retained condition.
(C) Retrograde transport is inhibited in *Shigella* infected cells. Hep2β cells were incubated for 1 hr at 19.5°C with StxBcy3 before the infection with M90T and *mxiD* bacteria for 15 min followed by incubation with TfA647 for 60 min at 37°C. After fixation and permeabilization, cells were labeled with anti-GM130 and anti-LPS. Scale bars represent 10 μm. (See also Figure S2.)

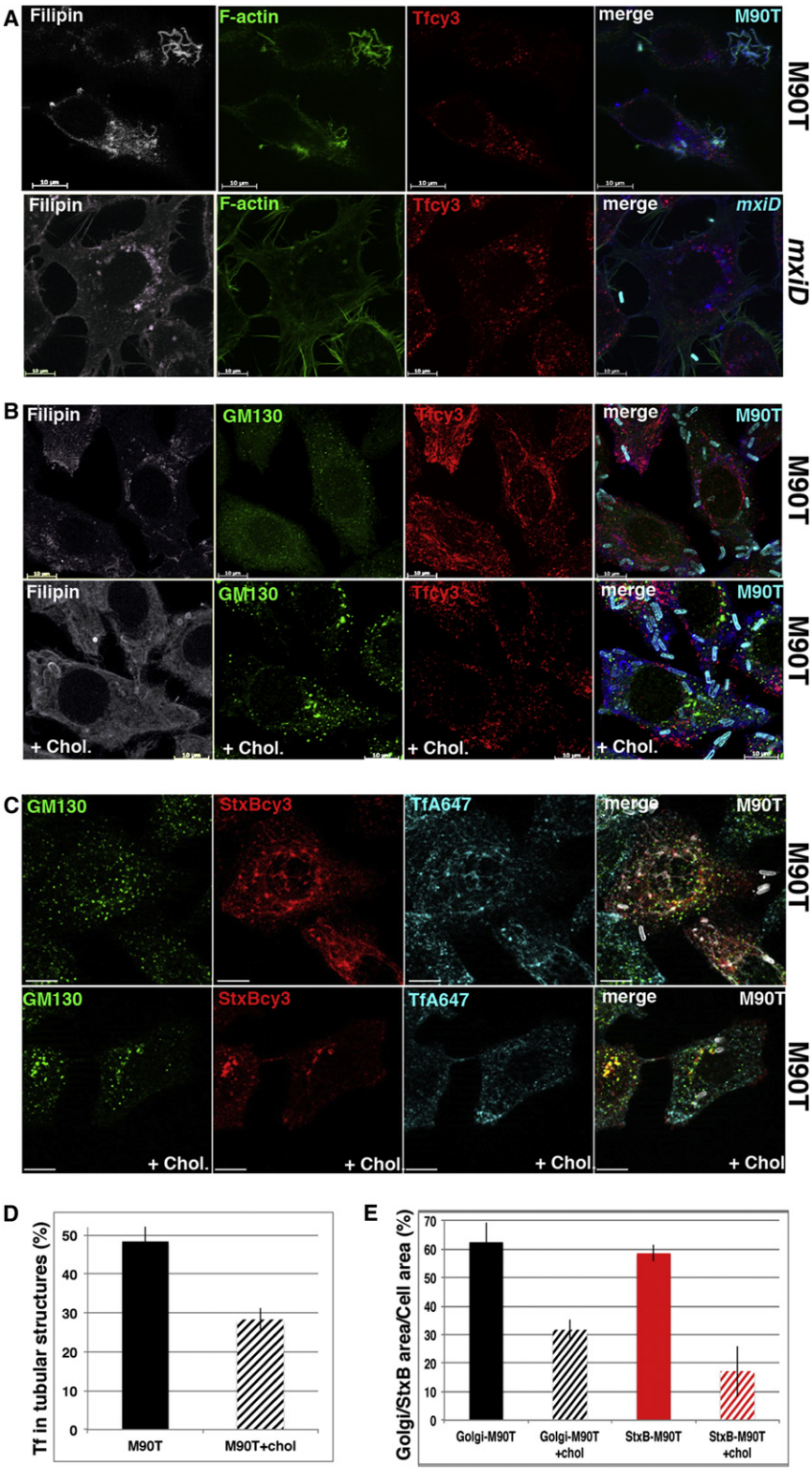

Figure 3. Distribution of Cholesterol during *Shigella* Infection

(A) Hep2β cells were infected with M90T or *mxiD* bacteria for 15 min at 37°C and Tfcy3 was added for 5 min at 37°C (20 min of infection). After fixation and permeabilization, cells were labeled with filipin, FITC-phalloidin and anti-LPS.

(B) Hep2β cells were infected with M90T or *mxiD* bacteria for 15 min at 37°C and Tfcy3 was added for 15 min at 37°C before adding (+ chol.) or not 10 mM of cholesterol for 30 min at 37°C (60 min of infection). After fixation and permeabilization, cells were labeled with filipin, anti-GM130 and anti-LPS.

(C) Hep2β cells were incubated for 1 hr at 19.5°C with StxBcy3 before the infection with M90T bacteria for 15 min followed by the incubation with TfA647 for 15 min at 37°C before adding (+ chol.) or not 10 mM of cholesterol for 30 min at 37°C (60 min of infection). After fixation and permeabilization, cells were labeled with anti-GM130 and anti-LPS. Scale bars represent 10 μm.

(D) Quantification of tubulated Tf using ICY from data presented in (B) (mean ± S.E.; n = 20).

(E) Quantification of the Golgi or StxB area using ICY on data presented in (B) and (C). The Golgi area is measured using GM130 labeling; the StxB area is measured using StxBcy3 labeling and expressed as a percentage of total cell area (mean ± S.E.; n = 20). (See also Figure S3.)

labeled by filipin, within the cell (Figure 4A). In control cells, cholesterol was associated to the cell surface and to the Golgi complex, while in IpaB-treated cells, numerous cholesterol-positive dotty structures were scattered inside the cell (Figure 4A).

Furthermore, IpaB incubation led to the fragmentation of the Golgi complex, occupying 56.6% of the cell area in contrast to control cells where it covered 9% of the cell area (Figures 4A and 4B). Thus, IpaB alone induces the Golgi dispersion. This IpaB-induced fragmentation was clearly linked to cholesterol. Indeed, sequestering the plasma membrane cholesterol before IpaB-incubation using β-methylcyclodextrin (βMCD) prevented IpaB-induced Golgi dispersion (Figures 4A and 4B). Compact Golgi complexes were found to be enriched in cholesterol as seen by filipin labeling. In βMCD-pretreated cells, IpaB distribution was different than in nonpretreated cells with most of the protein being found in large patches localized at the cell surface (Figure 4A). These results indicate that sequestering cholesterol abolished the effect of IpaB on Golgi dispersion. Furthermore, Golgi fragmentation was partially reverted by adding cholesterol to cells 30 min after IpaB incubation, as we observed a reduction of the Golgi area representing 27% of the cell area (Figures 4A and 4B). It is worth noting that the action of IpaB was temperature-dependent since no effect on the Golgi complex was observed upon

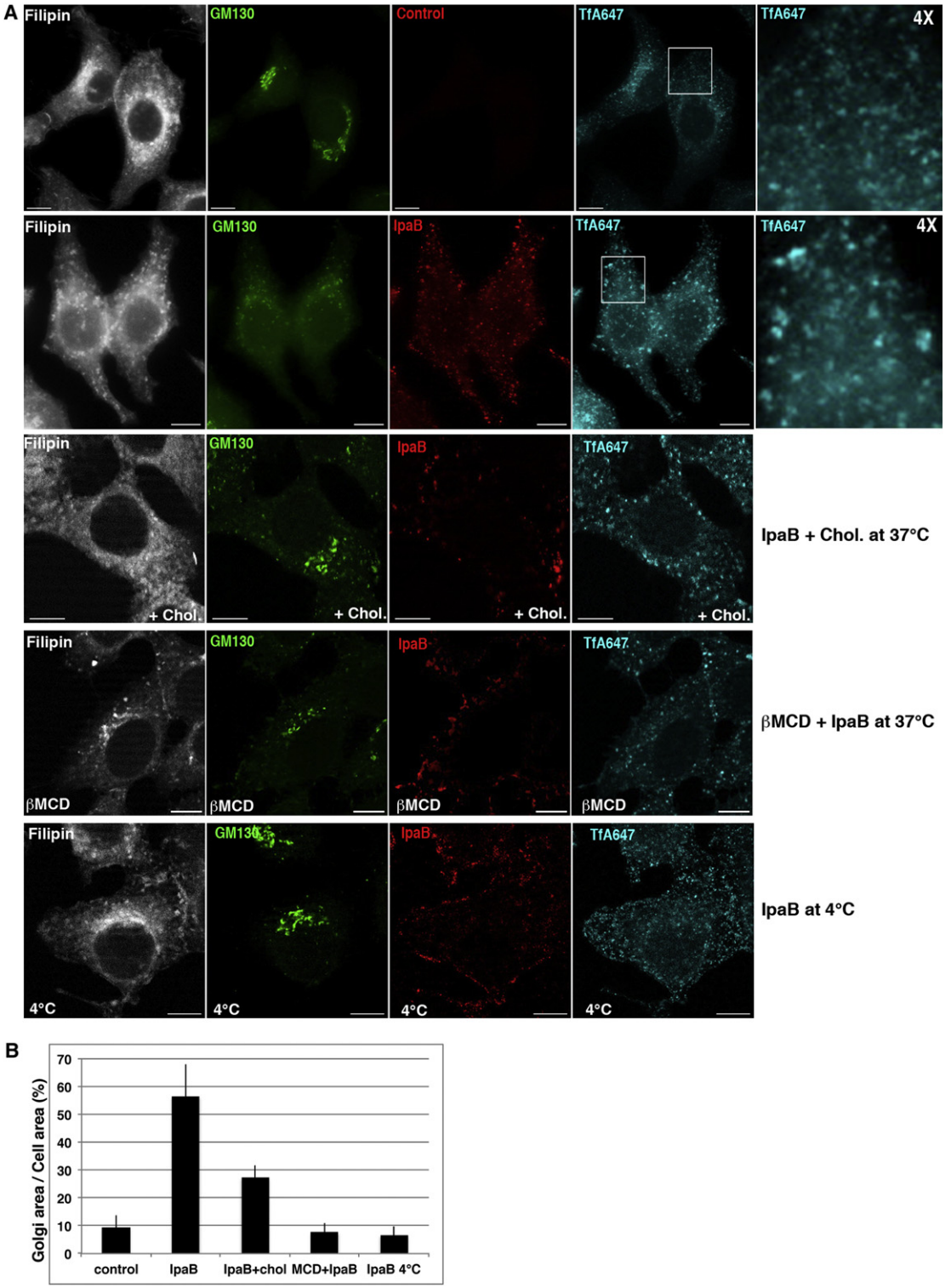

Figure 4. IpaB Induces the Reorganization of the Golgi-Recycling Network

(A) Hep2β cells were incubated with 400 nM of either IpaB or the elution buffer as a control, with TfA647 for 90 min at 37°C. After fixation and permeabilization, cells were labeled with filipin, anti-GM130, and anti-IpaB. On the right, details of Tf images are shown enlarged 4 times. Hep2β cells were either pretreated with 10 mM βMCD prior to incubation with 400 nM of IpaB and TfA647 for 90 min at 37°C (βMCD) or cells were first incubated for 30 min with 400 nM IpaB and TfA647 before adding 10 mM cholesterol for 60 min at 37°C (+ chol) or cells were incubated with 400 nM IpaB and TfA647 for 90 min at 4°C (4°C) before performing immunofluorescence experiment as described above. Scale bars represent 10 μm.

(B) Quantification of the Golgi area using ICY on data from A (mean ± S.E.; n = 25). (See also Figure S4.)

incubation at 4°C (Figures 4A and 4B). In this case, IpaB was found exclusively at the cell surface.

In addition, although we could not observe Tf-positive tubules in these IpaB-treated cells, recycling endosomes were larger than in control cells (see enlarged pictures of Tf in Figure 4A). Quantification of the data using the ICY software showed that Tf endosomes were 2 times bigger than in control cells, confirming an IpaB-induced reorganization of this compartment. Altogether, these data suggest that the cholesterol-binding protein of *Shigella*, IpaB, is responsible for the perturbation of the Golgi complex and, to a lesser extent, of recycling endosomes.

DISCUSSION

Pathogenic *Shigella* induces major reorganization and functional inhibition of the Golgi–TGN and recycling networks of its target epithelial cells by acting on cholesterol distribution. IpaB, a component of the T3SS translocator established in the plasma membrane is the responsible effector.

Even if *Shigella* quickly escapes into the cytoplasm following internalization (Ray et al., 2009; Sansonetti et al., 1986), it can affect key cellular compartments such as the recycling endosomes and the Golgi complex, regardless of the necessity to manage a survival niche in these compartments unlike *Salmonella* (Salcedo and Holden, 2003) or *Chlamydia* replicating in vacuoles and both disrupting the Golgi apparatus (Christian et al., 2011; Heuer et al., 2009).

In the case of *Shigella*, the morphological and functional alterations of both the recycling compartment and Golgi complex are striking and fast to appear. These modifications were also observed in vivo, thus they should affect epithelial functions in the course of invasion. Furthermore, integrity of the epithelial layer is maintained by strong cell-to-cell adhesion processes achieved by surface located E-cadherins (Solanas and Batlle, 2011). Our data demonstrating that E-cadherin trafficking to the plasma membrane is inhibited upon *Shigella* infection suggest that epithelial coherence and polarity may be severely affected as infection proceeds. Likewise, the morphological and functional destruction of the Golgi complex that is even observed in vivo is expected to strongly affect the maturation and secretion of key physiological and immunological mediators of antimicrobial defense normally localized at the cell surface (*i.e.* glycosylated receptors), or released in the extracellular milieu (i.e., cytokines and chemokines).

While it is clear that the effect of IpaB on Golgi dispersion is linked to cholesterol, the molecular mechanism underlying this process is not yet understood. As IpaB was shown to bind directly cholesterol, its action might be linked to this direct association. However, the total cholesterol content of the host cell is much higher than the number of IpaB molecules necessary to observe Golgi fragmentation, thereby excluding the sole effect of an IpaB-mediated cholesterol titration. On the other hand, IpaB binds to cholesterol molecules engaged in membrane microdomains raft (Lafont et al., 2002; Skoudy et al., 2000). This raft-mediated entry of *Shigella* requires that IpaB also interacts with the raft-associated protein CD44. Hence, IpaB could sequester the cholesterol content from raft domains often organized in signaling platforms linked to the cytoskeleton and other proteins that might be involved in Golgi and recycling compartments maintenance.

Also, as IpaB alone does not induce typical tubulation of recycling endosomes, we will try to identify if another factor of *Shigella* is involved in this process and try to understand why Rab11- and not Rab4-positive endosomes are tubulated upon *Shigella* infection.

Our present work also raises questions regarding the compartmentalization of eukaryotic cells. For instance, the actual mechanism of tubulation of recycling endosomes and disruption of the Golgi apparatus under cholesterol imbalance remains to be analyzed. Although cholesterol homeostasis is known to be important for Golgi function (Nhek et al., 2010; Wang et al., 2000), the mechanism by which cholesterol distribution interferes with endomembranes is not understood.

EXPERIMENTAL PROCEDURES

Bacterial Invasion, Immunofluorescence Assay and Fluorescent Microscopy

Bacteria were grown and freshly coated with poly-L-lysine before challenge to facilitate bacterial adhesion to cells. Bacteria were washed with PBS and resuspended with poly-L-lysine at a final concentration of 10 μg/ml in PBS. After 10 min incubation at room temperature, bacteria were washed 2 times with PBS, resuspended in DMEM containing 50 mM HEPES pH 7.4, and used immediately at a MOI of 50 bacteria / cell. Hep2β cells were plated at a density of 10^5 cells / 12 mm coverslip and washed twice with DMEM containing 50 mM HEPES pH 7.4 before infection. Bacteria were incubated onto cells for 15 min at room temperature, extracellular bacteria were removed and cells were incubated at 37°C for 15 min, before adding Tfcy3 or TfA647 in medium of internalization (MI) (DMEM-HEPES buffer with 0.1% BSA) for various time course at 37°C. Cells were then fixed with 4.7% paraformaldehyde (PFA) and 4% sucrose for 40 min, quenched with 50 mM NH_4Cl for 5 min and washed three times with PBS 0.1% BSA 0.05% saponin for permeabilization. Images in Z stacks of 0.24 μm were taken with an objective 63X, an Apotome microscope from Zeiss (slice of 0.7 μm), equipped with narrow filter sets for Dapi, GFP, DsRed and Cy5 (Zeiss) and a Roper Scientific Coolsnap HQ camera.

RUSH Assay to Assess Anterograde Trafficking

HeLa cells were transfected with the RUSH plasmid coding for Streptavidin-KDEL_SBP-EGFP-E-cadherin (Boncompain et al., 2012) using calcium phosphate method (Jordan et al., 1996). Twenty hours post transfection, cells were infected with M90T or *mxiD* bacteria as described above. After the 15 min of incubation at room temperature and 30 min at 37°C, the medium was replaced by medium containing 40 μM of biotin (Sigma). Cells were then fixed with PFA 3% for 15 min and immunofluorescence was performed as described above. Images were acquired on a Leica DM6000B epifluorescence microscope with a 63x objective and a Coolsnap HQ camera (Roper Scientific) with identical settings for the different coverslips. To determine the amount SBP-EGFP-E-cadherin present at the plasma membrane, after fixation cells were stained with an anti-GFP antibody (clones 7.1, Roche) and an anti-mouse Cy5 conjugated secondary antibody (Jackson Immunoresearch) prior to cell permeabilization. Regions corresponding to transfected and infected cells were drawn and the average intensity of the surface anti-GFP staining in these regions was quantified using MetaMorph. Identical regions were drawn to subtract background values. Values for at least 26 cells were normalized using values of cells without biotin and averaged (normalized fluorescence).

IpaB Purification and Incubation

Bacteria coexpressing *ipaB* and His tagged *ipgC* (chaperone of IpaB) (Lokareddy et al., 2010) were lysed using sonication in the presence of 20 mM sodium phosphate buffer (pH 7.4), 500 mM NaCl, 40 mM imidazole, 10 mM MgCl2 and 10% (v/v) glycerol (supplemented with protease inhibitor tablet and Dnase) and centrifuged. IpaB was separated from IpaB/IpgC complex in the supernatant using HisTrap HP column according to manufacturer instructions (Pharmacia) and further purified by size exclusion chromatography (HiLoad Superdex 200, Pharmacia) in buffer containing 20 mM HEPES (pH 7.4), 100 mM NaCl, 0.05% (w/w) Lauryldimethylamine *N*-oxide (LDAO)). We then

incubated Hep2β cells with 400 nM of IpaB or the elution buffer as a control and add TfA647 for 90 min at 37°C (or at 4°C when indicated). IpaB or the control medium, were also incubated onto cells pretreated 30 min before with 10 mM β-methylcyclodextrin (βMCD) to titrate cholesterol from plasma membrane. When specified 30 min after IpaB incubation, we added soluble cholesterol (10 mM) in "areal" medium without lipids for 60 min at 37°C. Cells were then fixed by PFA permeabilized, *cis*-Golgi labeled with anti GM130, cholesterol with filipin and IpaB stained with an anti-IpaB.

Additional experimental procedures are available in Supplemental Information.

SUPPLEMENTAL INFORMATION

Supplemental Information includes one movie, four figures, one table, Supplemental Experimental Procedures, and Supplemental References and can be found with this article online at http://dx.doi.org/10.1016/j.chom.2012.07.010.

ACKNOWLEDGMENTS

We are most grateful to Bruno Goud for the generous gift of valuable reagents and for advice on the manuscript. In addition, we thank Brice Sperandio and Samuel L. Stanley for the generous gift of human intestinal xenograft sections and Stéphanie Lebreton for advice, discussion, and the generous gift of reagent. We thank Valérie Malardé for technical help. We thank Fabrice de Chaumont and Nicolas Chenouard for valuable discussions. This work was partly funded by Programme Transversal de Recherche no. 387 from Institut Pasteur, the ERC advanced grant HOMEOEPITH, and a PR2 bilateral French-German grant of the French Ministry of Foreign Affairs to P.J.S. and the ANR "Blanc" to F.P.

Received: December 2, 2011
Revised: April 10, 2012
Accepted: July 5, 2012
Published: September 12, 2012

REFERENCES

Ashida, H., Ogawa, M., Mimuro, H., and Sasakawa, C. (2009). Shigella infection of intestinal epithelium and circumvention of the host innate defense system. Curr. Top. Microbiol. Immunol. *337*, 231–255.

Boncompain, G., Divoux, S., Gareil, N., de Forges, H., Lescure, A., Latreche, L., Mercanti, V., Jollivet, F., Raposo, G., and Perez, F. (2012). Synchronization of secretory protein traffic in populations of cells. Nat. Methods *9*, 493–498.

Christian, J.G., Heymann, J., Paschen, S.A., Vier, J., Schauenburg, L., Rupp, J., Meyer, T.F., Häcker, G., and Heuer, D. (2011). Targeting of a chlamydial protease impedes intracellular bacterial growth. PLoS Pathog. *7*, e1002283.

Clements, A., Smollett, K., Lee, S.F., Hartland, E.L., Lowe, M., and Frankel, G. (2011). EspG of enteropathogenic and enterohemorrhagic E. coli binds the Golgi matrix protein GM130 and disrupts the Golgi structure and function. Cell. Microbiol. *13*, 1429–1439.

Coumailleau, F., Das, V., Alcover, A., Raposo, G., Vandormael-Pournin, S., Le Bras, S., Baldacci, P., Dautry-Varsat, A., Babinet, C., and Cohen-Tannoudji, M. (2004). Over-expression of Rififylin, a new RING finger and FYVE-like domain-containing protein, inhibits recycling from the endocytic recycling compartment. Mol. Biol. Cell *15*, 4444–4456.

Epler, C.R., Dickenson, N.E., Olive, A.J., Picking, W.L., and Picking, W.D. (2009). Liposomes recruit IpaC to the Shigella flexneri type III secretion apparatus needle as a final step in secretion induction. Infect. Immun. *77*, 2754–2761.

Hayward, R.D., Cain, R.J., McGhie, E.J., Phillips, N., Garner, M.J., and Koronakis, V. (2005). Cholesterol binding by the bacterial type III translocon is essential for virulence effector delivery into mammalian cells. Mol. Microbiol. *56*, 590–603.

Heuer, D., Rejman Lipinski, A., Machuy, N., Karlas, A., Wehrens, A., Siedler, F., Brinkmann, V., and Meyer, T.F. (2009). Chlamydia causes fragmentation of the Golgi compartment to ensure reproduction. Nature *457*, 731–735.

Johannes, L., and Römer, W. (2010). Shiga toxins—from cell biology to biomedical applications. Nat. Rev. Microbiol. *8*, 105–116.

Jordan, M., Schallhorn, A., and Wurm, F.M. (1996). Transfecting mammalian cells: optimization of critical parameters affecting calcium-phosphate precipitate formation. Nucleic Acids Res. *24*, 596–601.

Lafont, F., Tran Van Nhieu, G., Hanada, K., Sansonetti, P., and van der Goot, F.G. (2002). Initial steps of Shigella infection depend on the cholesterol/sphingolipid raft-mediated CD44-IpaB interaction. EMBO J. *21*, 4449–4457.

Lebreton, S., Paladino, S., and Zurzolo, C. (2008). Selective roles for cholesterol and actin in compartmentalization of different proteins in the Golgi and plasma membrane of polarized cells. J. Biol. Chem. *283*, 29545–29553.

Lippincott-Schwartz, J., and Phair, R.D. (2010). Lipids and cholesterol as regulators of traffic in the endomembrane system. Annu Rev Biophys *39*, 559–578.

Lokareddy, R.K., Lunelli, M., Eilers, B., Wolter, V., and Kolbe, M. (2010). Combination of two separate binding domains defines stoichiometry between type III secretion system chaperone IpgC and translocator protein IpaB. J. Biol. Chem. *285*, 39965–39975.

Mallard, F., Antony, C., Tenza, D., Salamero, J., Goud, B., and Johannes, L. (1998). Direct pathway from early/recycling endosomes to the Golgi apparatus revealed through the study of shiga toxin B-fragment transport. J. Cell Biol. *143*, 973–990.

Mesmin, B., and Maxfield, F.R. (2009). Intracellular sterol dynamics. Biochim. Biophys. Acta *1791*, 636–645.

Nhek, S., Ngo, M., Yang, X., Ng, M.M., Field, S.J., Asara, J.M., Ridgway, N.D., and Toker, A. (2010). Regulation of oxysterol-binding protein Golgi localization through protein kinase D-mediated phosphorylation. Mol. Biol. Cell *21*, 2327–2337.

Parsot, C. (2009). Shigella type III secretion effectors: how, where, when, for what purposes? Curr. Opin. Microbiol. *12*, 110–116.

Phalipon, A., and Sansonetti, P.J. (2007). Shigella's ways of manipulating the host intestinal innate and adaptive immune system: a tool box for survival? Immunol. Cell Biol. *85*, 119–129.

Ray, K., Marteyn, B., Sansonetti, P.J., and Tang, C.M. (2009). Life on the inside: the intracellular lifestyle of cytosolic bacteria. Nat. Rev. Microbiol. *7*, 333–340.

Salcedo, S.P., and Holden, D.W. (2003). SseG, a virulence protein that targets Salmonella to the Golgi network. EMBO J. *22*, 5003–5014.

Sansonetti, P.J. (2006). The bacterial weaponry: lessons from Shigella. Ann. N Y Acad. Sci. *1072*, 307–312.

Sansonetti, P.J., Ryter, A., Clerc, P., Maurelli, A.T., and Mounier, J. (1986). Multiplication of Shigella flexneri within HeLa cells: lysis of the phagocytic vacuole and plasmid-mediated contact hemolysis. Infect. Immun. *51*, 461–469.

Selyunin, A.S., Sutton, S.E., Weigele, B.A., Reddick, L.E., Orchard, R.C., Bresson, S.M., Tomchick, D.R., and Alto, N.M. (2011). The assembly of a GTPase-kinase signalling complex by a bacterial catalytic scaffold. Nature *469*, 107–111.

Simons, K., and Ehehalt, R. (2002). Cholesterol, lipid rafts, and disease. J. Clin. Invest. *110*, 597–603.

Skoudy, A., Mounier, J., Aruffo, A., Ohayon, H., Gounon, P., Sansonetti, P., and Tran Van Nhieu, G. (2000). CD44 binds to the Shigella IpaB protein and participates in bacterial invasion of epithelial cells. Cellular microbiology *2*, 19–33.

Solanas, G., and Batlle, E. (2011). Control of cell adhesion and compartmentalization in the intestinal epithelium. Exp. Cell Res. *317*, 2695–2701.

Sperandio, B., Regnault, B., Guo, J., Zhang, Z., Stanley, S.L., Jr., Sansonetti, P.J., and Pédron, T. (2008). Virulent Shigella flexneri subverts the host innate immune response through manipulation of antimicrobial peptide gene expression. J. Exp. Med. *205*, 1121–1132.

Wang, Y., Thiele, C., and Huttner, W.B. (2000). Cholesterol is required for the formation of regulated and constitutive secretory vesicles from the trans-Golgi network. Traffic *1*, 952–962.